Title

Perivascular Mast Cells Dynamically Probe Cutaneous Blood Vessels to Capture Immunoglobulin E

Journal

Immunity, 38(1)

ISSN

1074-7613

Authors

Cheng, Laurence E

Hartmann, Karin

Roers, Axel

et al.

Publication Date

2013

DOI

10.1016/j.immuni.2012.09.022

Peer reviewed

Published in final edited form as:
Immunity. 2013 January 24; 38(1): 166–175. doi:10.1016/j.immuni.2012.09.022.

Perivascular mast cells dynamically probe cutaneous blood vessels to capture IgE

Laurence E. Cheng[1], **Karin Hartmann**[2], **Axel Roers**[3], **Matthew F. Krummel**[4], and **Richard M. Locksley**[5,6,7]

[1]Department of Pediatrics, University of California, San Francisco, San Francisco, CA 94143

[2]Department of Dermatology, University of Cologne, 50937 Cologne, Germany

[3]Institute for Immunology, University of Technology Dresden, Medical Faculty Carl-Gustav Carus, 01307 Dresden, Germany

[4]Department of Pathology, University of California, San Francisco, San Francisco, CA 94143

[5]Department of Medicine, University of California, San Francisco, San Francisco, CA 94143

[6]Department of Microbiology and Immunology, University of California, San Francisco, San Francisco, CA 94143

[7]Howard Hughes Medical Institute, University of California, San Francisco, San Francisco, CA 94143

SUMMARY

Mast cells are tissue-resident, immune cells that play a central role in allergic disease. These contributions are largely dependent on the acquisition of antigen-specific immunoglobulin E (IgE). Despite this requirement, studies of mast cell and IgE interactions have overlooked the mechanism by which mast cells acquire IgE from the blood. To address this gap, we developed reporter IgE molecules and employed imaging techniques to study mast cell function *in situ*. Our data demonstrate that skin mast cells exhibit selective uptake of IgE based on perivascular positioning. Furthermore, perivascular mast cells acquire IgE by extending cell processes across the vessel wall to capture luminal IgE. These data demonstrate how tissue mast cells acquire IgE and reveal a strategy by which extra-vascular cells monitor blood contents to capture molecules central to cellular function.

Introduction

Mast cells are hematopoietic, tissue-resident cells that have been considered to play diverse roles in host defense and immune regulation as well as a central role in allergic disease (Galli and Tsai, 2010; Gould and Sutton, 2008; Locksley, 2010). Despite these many potential roles, recent studies, using mouse strains with targeted mast cell deletion, have primarily served to underscore the mast cell contribution to the clinical manifestations of allergic disease (Dudeck et al., 2011; Feyerabend et al., 2011).

The mast cell contribution to allergy is largely dependent on the acquisition of monomeric IgE on the surface of mast cells through expression of the high affinity IgE receptor (FcεRI)

Corresponding author: Richard M. Locksley, 513 Parnassus Ave, Box 0795, San Francisco, CA 94143, locksley@medicine.ucsf.edu, Tel: (415) 476-5859, Fax: (415) 502-5081.

The authors declare no financial conflicts of interest.

(Kraft and Kinet, 2007). Though FcεRI can be detected on the surface of mast cell precursors (Hallgren and Gurish, 2007), expression of FcεRI on tissue-resident mast cells increases proportionally with serum IgE levels, suggesting the tissue as a primary site of IgE acquisition (Kraft and Kinet, 2007; Yamaguchi et al., 1997). Once mast cells are loaded with IgE, subsequent antigen binding leads to cross-linking of FcεRI molecules and the immediate release of pre-formed mediators, such as histamine, as well as synthesis of lipid and protein mediators (Galli and Tsai, 2010).

Studies of the mast cell-IgE axis have focused on the regulation of IgE production as well as the clinical manifestations of hypersensitivity responses following antigen exposure. Few studies have examined how mast cells acquire unbound IgE. Defining the mechanism by which mast cells capture IgE will fill a gap in our understanding of the mast cell-IgE axis and may provide new therapeutic approaches to severe allergic disorders.

Although cell-bound IgE is found primarily in tissues, IgE production by plasma cells occurs mostly in the bone marrow, spleen, and lymph nodes (Luger et al., 2009; McMenamin et al., 1992; Talay et al.; Yang et al.). Thus, the localization of IgE production is anatomically distinct from sites of IgE acquisition and effector function. As the amount of surface bound IgE by tissue mast cells directly reflects the size of the serum IgE pool (Kraft and Kinet, 2007), the vasculature acts as a conduit by which unbound IgE is distributed to tissue mast cells. The vasculature also acts as a potential barrier to IgE uptake and could thereby regulate IgE delivery to tissue sites.

Mast cells show a preference toward perivascular localization within tissue, wherein a majority of mast cells lie in close proximity to the basal side of the vessel wall (Galli and Tsai, 2010). We hypothesized that this preferential localization might position mast cells to acquire IgE by a mechanism that requires cells to surmount the endothelial barrier. Using reporter IgE molecules, *in vivo* imaging techniques, and mast cell reporter mice, we demonstrate that perivascular mast cells dynamically extend processes into the vascular compartment to selectively acquire IgE from the blood.

RESULTS

Heterogeneous IgE uptake by skin mast cells

Passive diffusion of blood-borne IgE across the vasculature has been considered to be the primary means by which tissue mast cells acquire IgE. However, we hypothesized a more active mechanism of IgE acquisition by mast cells, which would lead to selective uptake of IgE by a subset of mast cells. Supporting this idea, ear skin mast cells from 6-week old 4get BALB/c mice, in which mast cells constitutively express enhanced green fluorescent protein (eGFP) (Fig. S1 and Gessner et al., 2005), showed heterogeneous surface IgE levels with approximately 50% of the mast cells having high levels of IgE (Fig. 1A). In contrast, peritoneal mast cells exhibited uniform surface IgE levels. These differences were not a result of the protease-dependent skin mast cell isolation protocol as protease-treated peritoneal mast cells showed no loss of surface IgE (Fig. S2).

Mast cell-bound IgE has a half-life of up to 2 weeks and can modulate mast cell expression of FcεRI (Gould and Sutton, 2008; Yamaguchi et al., 1997). Therefore, we examined IgE uptake in IgE-deficient 4getxRag2$^{-/-}$ mice following intravenous (I.V.) infusion of 10 μg of IgE. Despite peak IgE levels more than 50-fold greater than physiologic levels in IgE-replete animals (*data not shown*), only a select population of ear skin mast cells demonstrated IgE uptake at 1 hour and continued to accumulate IgE throughout the time course (Fig. 1B). In contrast, peritoneal mast cells showed uniform uptake of IgE at one hour and further accumulation of IgE throughout the time course, similar to profiles seen at steady state in

wild-type animals. The ear skin mast cells also did not achieve surface IgE levels commensurate with peritoneal mast cells. Although slightly lower than on peritoneal mast cells, FcεRI expression on skin mast cells could not account for this discrepancy (Fig. 1C). Similar results were obtained with a smaller 1 μg infusion but with markedly lower IgE uptake in the ear (Fig. S3). Together, these data suggested that skin blood vessels regulate IgE trafficking into the tissue and that select mast cell populations had greater access to vascular contents. The data predicted that IgE uptake would similarly localize to perivascular mast cells.

Characterization of reporter IgE molecules and localization of IgE uptake

To visualize IgE uptake in tissues, we constructed a reporter IgE molecule consisting of a tandem Red Fluorescent Protein (tdRFP) fused N-terminal to the Cε2-4 domains of the IgE heavy chain (Cheng et al., 2010). The resulting homodimeric surrogate IgE molecule has a similar molecular weight as native IgE (188 kDa versus ~200 kDa for native IgE). After an I.V. infusion, RFP-Fcε was found on the cell surface of $FcεRI^+$ cells, including splenic basophils and peritoneal mast cells (Fig. 2A). Additionally, gating of peritoneal exudate cells and total splenocytes on RFP^+ cells revealed that essentially all of these cells were mast cells or basophils, respectively (Fig. 2B). Similar to data with native IgE, only a subset of skin mast cells captured RFP-Fcε after a 10 μg I.V. infusion (Fig. 2C). Together, these data indicated that RFP-Fcε displays similar binding and distribution characteristics to native IgE.

To visualize the distribution of mast cell IgE uptake, we infused 10 μg RFP-Fcε I.V. into wild-type or mast cell-deficient $W^{sh/sh}$ (Sash) mice (Wolters et al., 2005). After 24 hours, we counterstained blood vessels *in vivo* with I.V. tomato lectin FITC and examined whole mounts of ear tissue using confocal microscopy (Fig. 3A). Wild-type mice showed an abundance of RFP^+ cells with most cells lying in a perivascular location. In contrast to wild-type mice, mast cell-deficient mice demonstrated no RFP^+ cells in the ear skin, though RFP^+ basophils could be demonstrated within the vasculature (Fig. 3A). We next sought to obtain quantitative data to examine whether RFP^+ mast cells tended to be closer to blood vessels than the total mast cell pool. When bred to a *cre*-dependent lineage reporter mouse, such as Rosa-YFP (Srinivas et al., 2001), MCPT5cre reporter mice allow specific visualization of >90% of mast cells within the ear skin (Dudeck et al., 2011; Scholten et al., 2008). After infusion with RFP-Fcε, RFP-Fcε was found on ~50% of mast cells (Fig. 3B), and some $RFP\text{-}Fcε^+$ mast cells appeared to direct cellular projections toward the blood vessel though these initial studies lacked the resolution to define these projections (Fig 3C).

While $RFP\text{-}Fcε^+$ and $RFP\text{-}Fcε^-$ mast cells were both found to associate with the vasculature, RFP^+ mast cells were on average 35% closer to the nearest blood vessel compared to the total mast cell population (Fig. 3D). In addition, nearly half of the RFP^+ cells were within 2 μm of the nearest blood vessel, while only one quarter of the total mast cell population was similarly positioned (Fig. 3D). Together, these data indicated that perivascular mast cells preferentially acquire IgE from the blood, and we hypothesized that mast cells might directly sample blood to acquire IgE.

Perivascular mast cells have access to blood contents

We first took a flow cytometric approach to demonstrate that mast cells have direct access to blood contents. Similar to established approaches (Pereira et al., 2009; Zachariah and Cyster, 2010), we infused 4get mice with an anti-c-kit monoclonal antibody (2B8) conjugated to a high molecular weight fluorophore, phycoerythrin (PE). If allowed to circulate for a short period of time, PE-antibody conjugates remain intravascular and binding to target cells requires either direct blood exposure or sampling of intravascular contents.

After a 5-minute infusion, we observed that approximately 15–20% of mast cells captured 2B8-PE (Fig. 4A). Capture of 2B8-PE was not IgE-dependent as FcεRI$^{-/-}$ mice showed similar 2B8-PE uptake when compared to wild-type animals.

As noted in our prior experiments, peritoneal mast cells display rapid and uniform acquisition of IgE (Fig. 1). To examine whether peritoneal mast cells similarly display direct access to the blood, we assessed 2B8-PE binding in these cells. Consistent a lack of direct access to the blood and in contrast to ear skin mast cells, peritoneal mast cells showed no binding of 2B8-PE after I.V. exposure (Fig. 4B). This was not due to an inherent inability to bind this antibody as intraperitoneal injection of 2B8-PE led to rapid binding to peritoneal mast cells but essentially no binding to skin mast cells (Fig. 4B).

We next sought to characterize the positioning and dynamics of mast cell projections and blood vessels (Fig. 3B). To investigate this, we employed intravital, high-resolution confocal microscopy in MCPT5-cre × Ai6 mice (M5Ai6), which allowed for greater detail in visualization of mast cells and cellular projections *in vivo* (Madisen et al., 2010). Similar to our static imaging, we found mast cells closely approximated to blood vessels marked with labeled anti-CD31 antibody (Fig. 5A). We observed two distinct probing phenomena. First, some mast cells demonstrated relatively stable projections in the interior of blood vessels (Fig. 5A and Movie S1). As we followed such cells in time, serial images demonstrated the retraction of projections (Fig. 5B and Movie S2). In Figure 5B, the projection retracted approximately 5 μm over 30 minutes. We also noted a second behavior in which mast cells serially interacted with the vessel wall and/or the interior of the lumen with portions of the cell body or a cellular projection (Fig. 5C and Movie S3).

Although our data indicated that mast cell sampling of blood contents is an efficient means for perivascular mast cells to capture free IgE, other mechanisms could also contribute. Loading of monomeric IgE onto mast cells is thought to modulate mast cell function, including the possibility of piecemeal degranulation (Kawakami and Galli, 2002), which could lead to local changes in vasopermeability and increased IgE diffusion. Using cell surface CD107a and diminished side-scatter profile as markers of mast cell activation and degranulation, we examined whether IgE loading on mast cells resulted in changes in either of these parameters (Gekara and Weiss, 2008). To ensure uniform loading of mast cells during the assay, we used peritoneal mast cells as our source of mast cells. Following an IV infusion of IgE, peritoneal mast cells demonstrated baseline levels of CD107a and native SSC profiles, which contrasted with control antigen/IgE-activated mast cells (Fig. 6A). To directly address the importance of secreted mast cell products, such as histamine, on IgE uptake in skin, we used a pharmacologic approach to block H1 and H2 histamine receptors and mast cell degranulation. IgE loading in ear skin mast cells was not affected by these inhibitors (Fig. 6B).

We next wanted to determine whether mast cell projections directly interact with intravascular IgE. As fluorescence of RFP-Fcε was too insensitive for this application, we developed a technique using streptavidin-coated beads coupled to biotinylated IgE and a fluorescent dye. After an infusion of 10^9 beads, beads were found in systemic circulation but were cleared within 15 minutes (*data not shown*). As a control, we used dye-coated beads. After infusion of control beads into mast cell reporter mice, we found a few beads near perivascular mast cells but no interaction with the bead (Fig. 7A and Movie S4). In contrast, mast cells showed interactions with IgE-coated beads in the form of projections extending toward an intravascular bead and engulfing it (Fig. 7B and Movie S5 and S6).

To further establish the capacity of mast cells to capture intravascular IgE, we determined the number of IgE-coated beads in mouse ear skin 20 minutes after infusion. In mast cell

replete mice, we recovered an average of 1337 beads per mg of ear tissue (Fig. 7C). In contrast, mast cell deficient (MCPT5cre × Rosa-DTA) mice exhibited a nearly 70% drop in bead recovery. Together, these data indicate that mast cells interact directly with intravascular contents in a dynamic fashion and selectively remove IgE from blood.

DISCUSSION

The acquisition of IgE by mast cells is central to mast cell function, and the importance of this interaction has been underscored by two recent studies (Dudeck et al., 2011; Feyerabend et al., 2011). Given the critical role of IgE in mast cell biology, our study sought to examine how tissue mast cells acquire IgE. The studies presented here indicate that IgE acquisition by mast cells is regulated at the level of the vasculature with perivascular mast cells demonstrating selective uptake of IgE from the blood.

Immune surveillance of intravascular components has been previously described in professional antigen presenting cells (APC), including intra-aortic dendritic cells and Kupffer cells, which also reside within the vasculature (Choi et al., 2009; Lee et al., 2010). Our data illustrate that extravascular cells are also capable of probing blood, akin to sampling of intraluminal contents in the gastrointestinal and respiratory tracts by $CD103^{+}$ dendritic cells (Chieppa et al., 2006; Lambrecht and Hammad, 2009; Rescigno et al., 2001). Mast cells are not generally considered to be antigen presenting cells, though mast cells may express MHC class II under specific conditions (Kambayashi et al., 2009). Instead, intravascular sampling appears to be a means for mast cells to capture unbound IgE, which in turn could promote mast cell function and survival (Kawakami and Galli, 2002; Kraft and Kinet, 2007).

Tissue mast cells have long been known to project dendrites, although the function of these projections has not been clear. Beyond sampling blood, mast cells may also extend projections for intercellular communication through a network of cytonemes. The significance of these projections has not been examined *in vivo* (Fifadara et al., 2010).

We speculate that in addition to capturing IgE, mast cells employ this sampling mechanism as part of a sentinel function in host defense. Localization to barrier surfaces, the capacity to induce immediate inflammatory responses, and the ability to recruit additional immune cells, positions mast cells as initial responders to pathogen invasion. Specific IgE further enhances these functions when antigen is present. Although local production of IgE has been described in the airway mucosa (Gould and Sutton, 2008), delivery to the skin and mucosal sites remote from IgE production requires systemic distribution. The surveillance mechanism we describe limits distribution of IgE to subsets of mast cells in close approximation to the vasculature. Thus, the cells most likely to influence vascular permeability after activation also have the greatest access to free IgE. It remains unclear whether this anatomic positioning also defines subsets of mast cells that have functional differences beyond the effects of IgE.

Our studies focus on the steady state means by which mast cells acquire IgE. Local changes in vascular permeability, which could be seen with immediate hypersensitivity reactions, infection, or dermatitis, may further modulate IgE loading. In addition, the disparate mechanisms by which skin and peritoneal mast cells acquire IgE suggest that IgE uptake may be organ-specific. Several factors, including mast cell positioning, local vascular permeability, and the predominant mast cell populations (connective tissue versus mucosal) contained within each organ may all play a role in IgE acquisition.

Our data uncover a regulated means by which mast cells acquire IgE and fill an important gap in our understanding of the steps required in the elicitation of hypersensitivity by mast

cells. The molecular mechanism by which mast cells survey blood remains undefined. We hypothesize that a gradient between blood and tissue levels of a particular factor or family of molecules may drive mast cell sampling behavior. Further understanding of the mechanism by which mast cells survey the blood compartment may provide a means to modulate human allergic disease in the future.

EXPERIMENTAL PROCEDURES

Mice

4get BALB/c and IgE-deficient 4getxRag2$^{-/-}$ mice have been described (Cheng et al., 2010; Mohrs et al., 2001). Mast cell-deficient W^{sh}/W^{sh} (Sash) mice on a C57BL/6 background were provided by G. Caughey (UCSF). MCPT5 cre mice were bred to either of the following reporter mice: Rosa-YFP, Ai6, or Rosa-DTA (Madisen et al., 2010; Srinivas et al., 2001; Voehringer et al., 2008). Rosa-YFP and Ai6 mice were obtained from Jackson Laboratories (Bar Harbor, ME). Mice were housed in Specific Pathogen Free facilities. Experimental mice were 6–10 weeks old. Animal use was governed by and in accordance with approved protocols overseen by the Laboratory Animal Resource Center (LARC) and Institutional Animal Care and Use Committee (IACUC) at UCSF.

Skin tissue and peritoneal mast cell isolation

Ear tissue from euthanized mice was split into dorsal and ventral halves, and then minced. Tissue was re-suspended in PBS plus 2 U/ml of Liberase CI (Roche) and incubated at 37°C for 45 minutes in an orbital shaker similar to published protocols (Grimbaldeston et al., 2007). Collagenase activity was quenched with PBS supplemented with 2% fetal calf serum (FCS), and the cells analyzed by flow cytometry. Peritoneal mast cells were analyzed from lavage fluid collected after euthanasia. The gating scheme was similar to a previously published study (Gessner et al., 2005).

Construction of RFP-Fcε

RFP-Fcε was constructed and produced in the same manner as previous molecules (Cheng et al., 2010). A primer pair (5’- TTTAGATCTGTGAGCAAGGGCGAGG-3’ and 5’-TGGATCCCTTGTACAGCTCGTCCATGC-3’) that spanned amino acids 2–476 was used to amplify the tdRFP cDNA (Shaner et al., 2004).

Antibodies and flow cytometry

For mast cell staining, we used the following antibody clones: c-kit (ACK2, eBioscience, San Diego, CA), FcεRI (Mar-1, eBioscience). For basophil staining, we used: CD49b (DX5, eBioscience). For *in vivo* infusion, the following antibodies and clones were used: mouse IgE C38-2 (BD Pharmingen, San Diego, CA) anti-CD31 APC (390, eBioscience), tomato lectin FITC (Vector Labs, Burlingame, CA), anti-c-kit PE (2B8, eBioscience). For flow cytometry, we used an LSRII (Becton-Dickinson, San Jose, CA) for data acquisition and analysis. We performed post-acquisition analysis using FlowJo software (Treestar, Ashland, OR).

Mast cell blood sampling

One μg of PE-conjugated 2B8 or isotype control rat IgG2b antibody were infused I.V. into the tail veins of mice. Within five minutes, mice were euthanized with immediate processing of tissue for flow cytometry. Statistical analysis was performed using an unpaired *t* test.

Confocal microscopy

For confocal microscopy, ear tissue from euthanized mice was split into dorsal and ventral halves (except for experiments involving bead infusions for which the ears remained intact). The tissue was then bathed in Vectashield (Vector Labs) and analyzed with a Nikon C1si laser scanning confocal microscope. Images were analyzed and rendered using Imaris software (Bitplane, Zurich, Switzerland). To analyze the distance from mast cells to blood vessels, we used Imaris software to mark the boundaries of the blood vessels and to generate "spots" to represent index populations. The software then calculated the distance from the center of each of these spots to the edge of the nearest blood vessel. A students *t*-test was performed for significance on the resulting data sets.

Intravital microscopy

Mice received intraperitoneal injections of ketamine and xylazine for anesthesia. Mice were then placed in a lateral decubitus position on the imaging stage of a Nikon C1si microscope. The ventral half of the ear was then dissected away with preservation of blood flow to the dorsal half verified under light microscopy. The mouse was then secured on the stage with the microscope objective directed toward the dermal surface. Images were compiled, analyzed, and rendered using Imaris software (Bitplane, Zurich, Switzerland).

IgE Beads

Monoclonal, anti-trinitrophenol IgE (C38-2) was biotinylated with EZ-Link Sulfo NHS (Thermo Scientific, Rockford, IL). After purification (Zeba Spin Desalting columns, Thermo Scientific), 40 μg of IgE (4B12, Vector Labs) was then combined with ~10^9 Dynal MyOne T1 streptavidin beads for 15 minutes (Invitrogen, Carlsbad, CA). To quench unoccupied streptavidin moieties and label the bead, 40 μg of dextran (3 kDa) coupled to biotin and tetramethylrhodamine was added to the mixture for 15 minutes (Invitrogen). The beads were then washed and resuspended in PBS prior to I.V. infusion. Ten minutes after infusion, ears were dissected from euthanized mice and analyzed intact using confocal microscopy. For the bead recovery assay, ears were harvested 20 minutes after infusion, weighed, and placed directly into digest buffer (0.25% SDS, 0.1 M NaCl, 50mM Tris pH 8, 7.5 mM EDTA) with an additional 0.5 mg/ml Proteinase K for 3 hours at 56 degrees and constant agitation. Magnetic beads were then isolated using a Dynal magnet (Invitrogen, Carlsbad, CA) after multiple washes with PBS and resuspended in 100 ul of water. The beads were then counted manually with a hemacytometer.

LAMP-1 staining

Four hours after I.V. IgE infusion or IP challenge with 1 mg of TNP-ovalbumin in sensitized animals, peritoneal lavage fluid was isolated and $ckit^+GFP^+$ mast cells were stained with anti-CD107a (1D4B, eBioscience).

Histamine blockade and cromolyn sodium administration

Mice received inhibitors of mast cell degranulation (cromolyn) and histamine blockade per published protocols (Dawicki et al., 2010).

Supplementary Material

Refer to Web version on PubMed Central for supplementary material.

Acknowledgments

This work was supported by the following grants to RML: the Howard Hughes Medical Institute, NIH AI026918, AI30663, AI078869, SABRE Center at UCSF and the following grants to LEC: NIH T32 (HD044331), AAAAI-GSK Career Development award, the A.P. Giannini Medical Research Foundation, and NIH AI095319. We thank Chris Allen and George Caughey for providing mice, and the Biological Imaging Development Center for assistance with microscopy. We thank members of the Locksley laboratory, Chris Allen, Jason Cyster, and Shaun Coughlin for thoughtful discussions and/or review of the manuscript. We also thank Paul Kubes for sharing experimental protocols.

REFERENCES

Cheng LE, Wang Z, Locksley RM. Murine B cells regulate serum IgE levels in a CD23- dependent manner. J Immunol. 2010:8.

Chieppa M, Rescigno M, Huang AY, Germain RN. Dynamic imaging of dendritic cell extension into the small bowel lumen in response to epithelial cell TLR engagement. J Exp Med. 2006; 203:2841–2852. [PubMed: 17145958]

Choi JH, Do Y, Cheong C, Koh H, Boscardin SB, Oh YS, Bozzacco L, Trumpfheller C, Park CG, Steinman RM. Identification of antigen-presenting dendritic cells in mouse aorta and cardiac valves. J Exp Med. 2009; 206:497–505. [PubMed: 19221394]

Dawicki W, Jawdat DW, Xu N, Marshall JS. Mast cells, histamine, and IL-6 regulate the selective influx of dendritic cell subsets into an inflamed lymph node. J Immunol. 2010; 184:2116–2123. [PubMed: 20083654]

Dudeck A, Dudeck J, Scholten J, Petzold A, Surianarayanan S, Kohler A, Peschke K, Vohringer D, Waskow C, Krieg T, et al. Mast cells are key promoters of contact allergy that mediate the adjuvant effects of haptens. Immunity. 2011; 34:973–984. [PubMed: 21703544]

Feyerabend TB, Weiser A, Tietz A, Stassen M, Harris N, Kopf M, Radermacher P, Moller P, Benoist C, Mathis D, et al. Cre-Mediated Cell Ablation Contests Mast Cell Contribution in Models of Antibody- and T Cell-Mediated Autoimmunity. Immunity. 2011

Fifadara NH, Beer F, Ono S, Ono SJ. Interaction between activated chemokine receptor 1 and FcepsilonRI at membrane rafts promotes communication and F-actin-rich cytoneme extensions between mast cells. Int Immunol. 2010; 22:113–128. [PubMed: 20173038]

Galli SJ, Tsai M. Mast cells in allergy and infection: Versatile effector and regulatory cells in innate and adaptive immunity. Eur J Immunol. 2010; 40:1843–1851. [PubMed: 20583030]

Gekara NO, Weiss S. Mast cells initiate early anti-Listeria host defences. Cell Microbiol. 2008; 10:225–236. [PubMed: 17714516]

Gessner A, Mohrs K, Mohrs M. Mast cells, basophils, and eosinophils acquire constitutive IL-4 and IL-13 transcripts during lineage differentiation that are sufficient for rapid cytokine production. J Immunol. 2005; 174:1063–1072. [PubMed: 15634931]

Gould HJ, Sutton BJ. IgE in allergy and asthma today. Nat Rev Immunol. 2008; 8:205–217. [PubMed: 18301424]

Grimbaldeston MA, Nakae S, Kalesnikoff J, Tsai M, Galli SJ. Mast cell-derived interleukin 10 limits skin pathology in contact dermatitis and chronic irradiation with ultraviolet B. Nat Immunol. 2007; 8:1095–1104. [PubMed: 17767162]

Hallgren J, Gurish MF. Pathways of murine mast cell development and trafficking: tracking the roots and routes of the mast cell. Immunol Rev. 2007; 217:8–18. [PubMed: 17498048]

Kambayashi T, Allenspach EJ, Chang JT, Zou T, Shoag JE, Reiner SL, Caton AJ, Koretzky GA. Inducible MHC class II expression by mast cells supports effector and regulatory T cell activation. J Immunol. 2009; 182:4686–4695. [PubMed: 19342644]

Kawakami T, Galli SJ. Regulation of mast-cell and basophil function and survival by IgE. Nat Rev Immunol. 2002; 2:773–786. [PubMed: 12360215]

Kraft S, Kinet JP. New developments in FcepsilonRI regulation, function and inhibition. Nat Rev Immunol. 2007; 7:365–378. [PubMed: 17438574]

Lambrecht BN, Hammad H. Biology of lung dendritic cells at the origin of asthma. Immunity. 2009; 31:412–424. [PubMed: 19766084]

Lee WY, Moriarty TJ, Wong CH, Zhou H, Strieter RM, van Rooijen N, Chaconas G, Kubes P. An intravascular immune response to Borrelia burgdorferi involves Kupffer cells and iNKT cells. Nat Immunol. 2010; 11:295–302. [PubMed: 20228796]

Locksley RM. Asthma and allergic inflammation. Cell. 2010; 140:777–783. [PubMed: 20303868]

Luger EO, Fokuhl V, Wegmann M, Abram M, Tillack K, Achatz G, Manz RA, Worm M, Radbruch A, Renz H. Induction of long-lived allergen-specific plasma cells by mucosal allergen challenge. J Allergy Clin Immunol. 2009; 124:819–826. e814. [PubMed: 19815119]

Madisen L, Zwingman TA, Sunkin SM, Oh SW, Zariwala HA, Gu H, Ng LL, Palmiter RD, Hawrylycz MJ, Jones AR, et al. A robust and high-throughput Cre reporting and characterization system for the whole mouse brain. Nat Neurosci. 2010; 13:133–140. [PubMed: 20023653]

McMenamin C, Girn B, Holt PG. The distribution of IgE plasma cells in lymphoid and non-lymphoid tissues of high-IgE responder rats: differential localization of antigen-specific and 'bystander' components of the IgE response to inhaled antigen. Immunology. 1992; 77:592–596. [PubMed: 1283601]

Mohrs M, Shinkai K, Mohrs K, Locksley RM. Analysis of type 2 immunity in vivo with a bicistronic IL-4 reporter. Immunity. 2001; 15:303–311. [PubMed: 11520464]

Pereira JP, An J, Xu Y, Huang Y, Cyster JG. Cannabinoid receptor 2 mediates the retention of immature B cells in bone marrow sinusoids. Nat Immunol. 2009; 10:403–411. [PubMed: 19252491]

Rescigno M, Urbano M, Valzasina B, Francolini M, Rotta G, Bonasio R, Granucci F, Kraehenbuhl JP, Ricciardi-Castagnoli P. Dendritic cells express tight junction proteins and penetrate gut epithelial monolayers to sample bacteria. Nat Immunol. 2001; 2:361–367. [PubMed: 11276208]

Scholten J, Hartmann K, Gerbaulet A, Krieg T, Muller W, Testa G, Roers A. Mast cell-specific Cre/loxP-mediated recombination in vivo. Transgenic Res. 2008; 17:307–315. [PubMed: 17972156]

Shaner NC, Campbell RE, Steinbach PA, Giepmans BN, Palmer AE, Tsien RY. Improved monomeric red, orange and yellow fluorescent proteins derived from Discosoma sp. red fluorescent protein. Nat Biotechnol. 2004; 22:1567–1572. [PubMed: 15558047]

Srinivas S, Watanabe T, Lin CS, William CM, Tanabe Y, Jessell TM, Costantini F. Cre reporter strains produced by targeted insertion of EYFP and ECFP into the ROSA26 locus. BMC Dev Biol. 2001; 1:4. [PubMed: 11299042]

Talay O, Yan D, Brightbill HD, Straney EE, Zhou M, Ladi E, Lee WP, Egen JG, Austin CD, Xu M, Wu LC. IgE memory B cells and plasma cells generated through a germinalcenter pathway. Nat Immunol. 2012; 13:396–404. [PubMed: 22366892]

Voehringer D, Liang HE, Locksley RM. Homeostasis and effector function of lymphopenia-induced"memory-like" T cells in constitutively T cell-depleted mice. J Immunol. 2008; 180:4742–4753. [PubMed: 18354198]

Wolters PJ, Mallen-St Clair J, Lewis CC, Villalta SA, Baluk P, Erle DJ, Caughey GH. Tissue-selective mast cell reconstitution and differential lung gene expression in mast celldeficient Kit(W-sh)/Kit(W-sh) sash mice. Clin Exp Allergy. 2005; 35:82–88. [PubMed: 15649271]

Yamaguchi M, Lantz CS, Oettgen HC, Katona IM, Fleming T, Miyajima I, Kinet JP, Galli SJ. IgE enhances mouse mast cell Fc(epsilon)RI expression in vitro and in vivo: evidence for a novel amplification mechanism in IgE-dependent reactions. J Exp Med. 1997; 185:663–672. [PubMed: 9034145]

Yang Z, Sullivan BM, Allen CD. Fluorescent In Vivo Detection Reveals that IgE(+) B Cells Are Restrained by an Intrinsic Cell Fate Predisposition. Immunity. 2012

Zachariah MA, Cyster JG. Neural crest-derived pericytes promote egress of mature thymocytes at the corticomedullary junction. Science. 2010; 328:1129–1135. [PubMed: 20413455]

HIGHLIGHTS

- Skin mast cells exhibit selective uptake of IgE from the blood
- Selective uptake is localized to perivascular mast cells
- Mast cells extend cellular processes to survey vascular contents and capture IgE

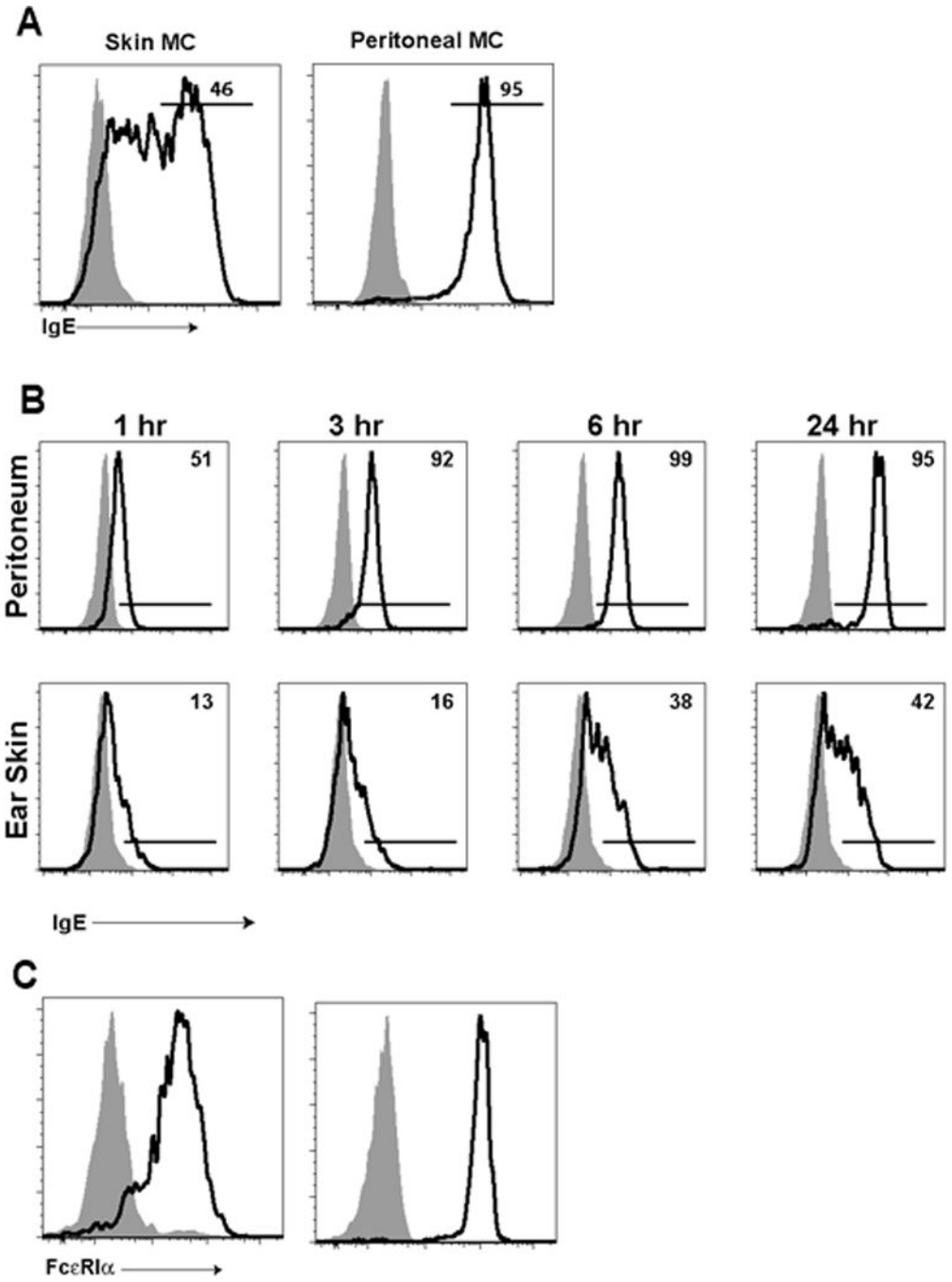

Figure 1. Heterogeneous uptake of IgE from blood by skin mast cells

A. Skin (left panel) and peritoneal (right panel) mast cells from 4get BALB/c mice were stained for IgE. Gray histograms represent IgE staining on mast cells from IgE-deficient 4getxRag2$^{-/-}$ controls. Lines within histograms represent the percent of cells within the indicated gate.

B. Peritoneal (top row) and ear skin mast cells (bottom row) from 4getRag2$^{-/-}$ mice were examined at the indicated times following a 10 μg I.V. infusion of monoclonal IgE. Histograms depict mast cell surface IgE. Shaded histograms represent control mice. The percent of IgE^{+} cells in the gated area of the histogram is also depicted.

These data are representative of 3 independent experiments with 2–3 mice at each time point.

C. IgE-deficient 4getxRag2$^{-/-}$ mast cells were stained with anti-FcεRI antibody. Gray histograms represent the isotype control. Results are representative of 3 mice for each plot.

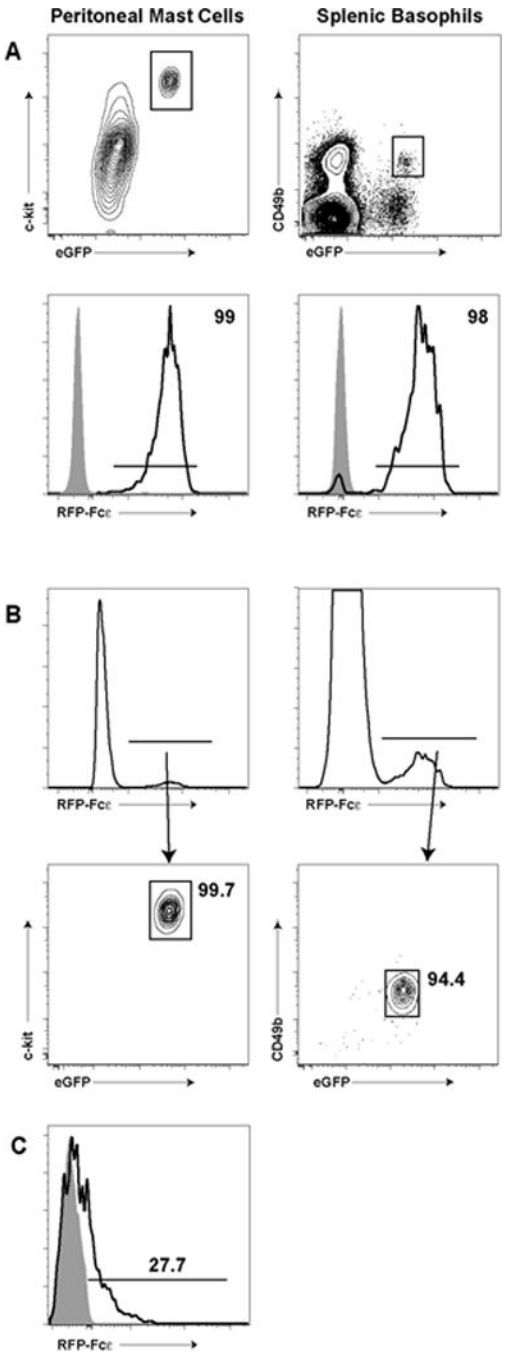

Figure 2. Characterization of RFP-Fcε

A) and B) We isolated peritoneal mast cells (left column) and splenic basophils (right column) from 4get BALB/c mice infused with 1 μg of RFP-Fcε I.V. one day prior. In A), we gated for c-kit$^+$GFP$^+$ mast cells and CD49b$^+$GFP$^+$ basophils and examined RFP-Fcε capture (bottom row, black histograms). Gray histograms represent similarly gated cells from non-infused mice. In B), we took total live cells from the peritoneum (left column) or spleen (right column) and analyzed all RFP$^+$ cells. RFP$^+$ cells were then gated on c-kit$^+$GFP$^+$ mast cells (left contour plot) and CD49b$^+$GFP$^+$ basophils (right

contour plot). The percent of cells lying in the respective gate is noted in the contour plots.

C) We isolated ckit^{+}GFP^{+} skin mast cells from 4get BALB/c mice one day following an I.V. 10 μg RFP-Fcε infusion. The black histogram represents the percent RFP^{+} cells within the indicated gate. The gray histogram represents RFP fluorescence from a non-infused animal.

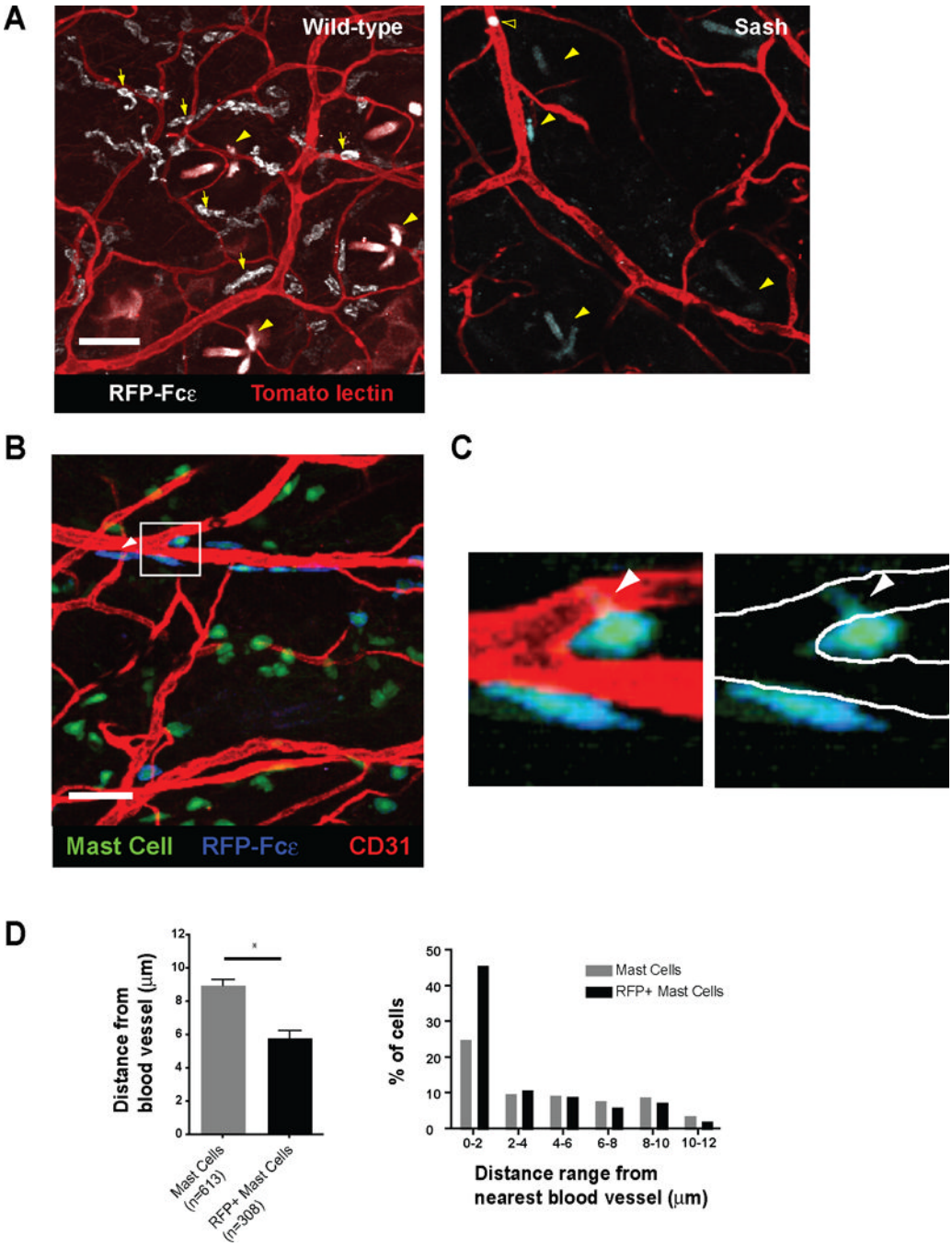

Figure 3. Perivascular mast cells preferentially capture RFP-Fcε from blood *in situ*

A. Wild-type or mast cell-deficient (Sash) mice received 10 μg of RFP-Fcε I.V. and were analyzed for RFP-Fcε uptake by confocal microscopy 24 hours later. Images represent 12 and 15 μm z-projections from whole mounts of ear tissue. Yellow arrows highlight representative RFP^+ mast cells, yellow arrowheads indicate hair follicles, and the open arrowhead in the right panel indicates a basophil. Tomato lectin was used to counterstain blood vessels. Images representative of results from 8 separate mice. Scale bars represent 50 μm.

B. A maximum intensity projection derived from a 24 μm z-stack of ear skin from a M5cre × Rosa-YFP mouse. The mouse received 10 μg of RFP-Fcε I.V. one day prior and anti-CD31 blood vessel counterstain 10 minutes prior to analysis. Scale bars indicate 50 μm. The white arrowhead highlights a YFP^+ mast cell with peripheral RFP-Fcε in blue. Images are representative of 10 individual z-stacks.

C. The left panel represents a zoomed in view of the box in 3B. In the right panel, the borders of the blood vessel wall are denoted by white lines with the green projection of the mast cell body within the boundaries of the vessel wall.

D. Total YFP^+ mast cells or RFP^+ mast cells from M5cre × Rosa-YFP mice that had received 10 μg of RFP-Fcε I.V. one day prior were examined for mean distance from the nearest blood vessel, using an imaging analysis tool. The left panel depicts the average distance of the indicated mast cell population from the nearest blood vessel, and the right panel represents the percent of mast cells within the indicated distance range from the nearest blood vessel. Four z-stacks were analyzed with a total of 613 YFP^+ mast cells and 308 RFP^+ mast cells. Graph in left panel depicts mean ± SEM. *$p<0.0001$

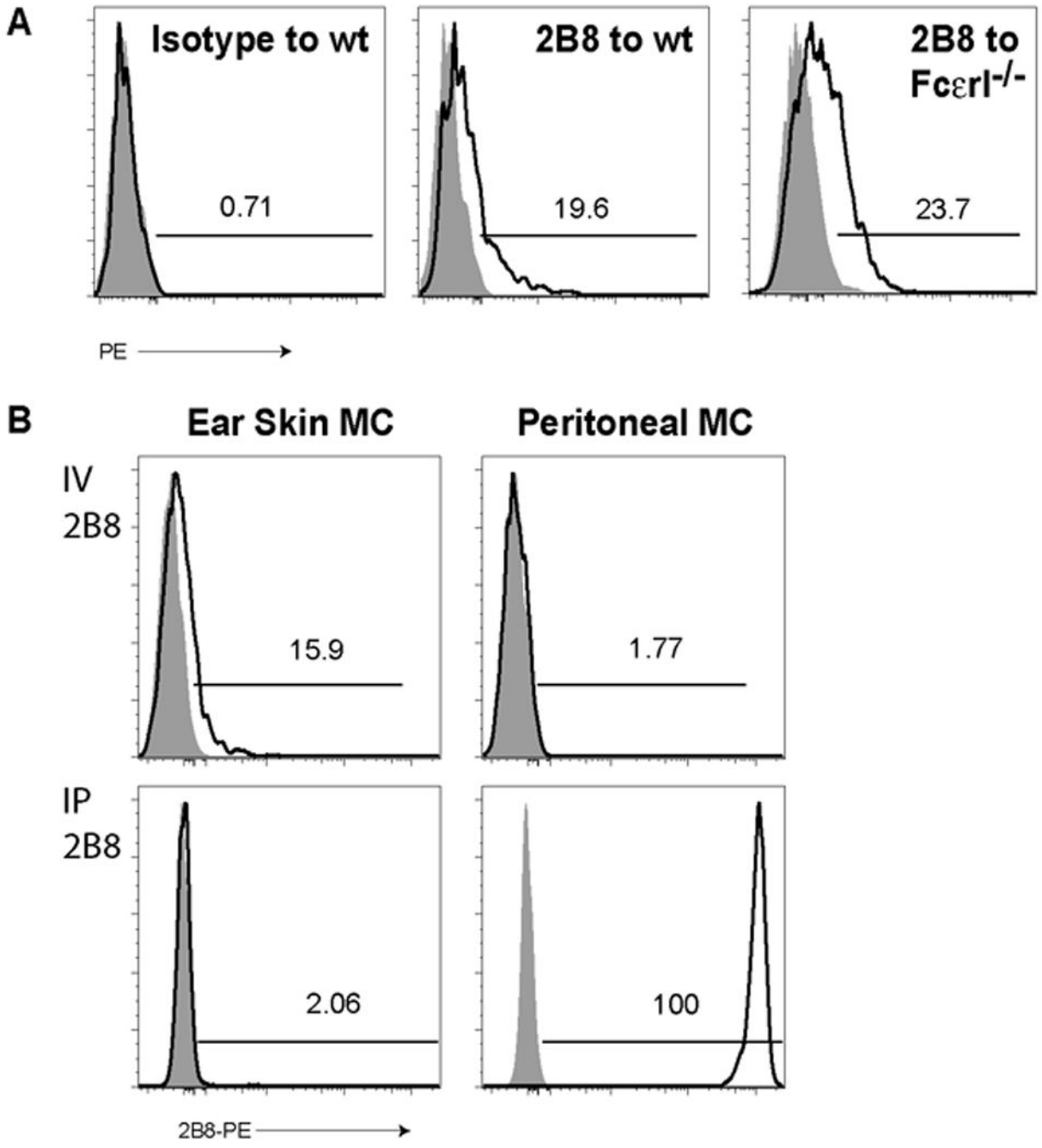

Figure 4. Mast cells probe blood to access serum contents

A. Within five minutes after I.V. injection of isotype control (left panel) or 2B8 (middle and right panels) antibodies conjugated to PE, we examined c-kit^{+}GFP^{+} ear skin mast cells for antibody uptake in wild-type (left and middle panels) or FcεRI$^{-/-}$ animals (right panel) from 4get BALB/c mice. Data are representative of 3 experiments with 2–6 samples per group. Numbers represent the percent of PE positive cells in each sample. Shaded histograms represent mice that did not receive labeled antibody.

B. 4get BALB/c mice received 2B8-PE either I.V. (top row) or I.P. (bottom row), and 5 minutes later, we examined ear skin (left column) or peritoneal (right column) mast cells for 2B8-PE uptake (black histograms). Gray histograms depict non-infused animals. The percent of cells within the indicated gates are depicted within each plot.

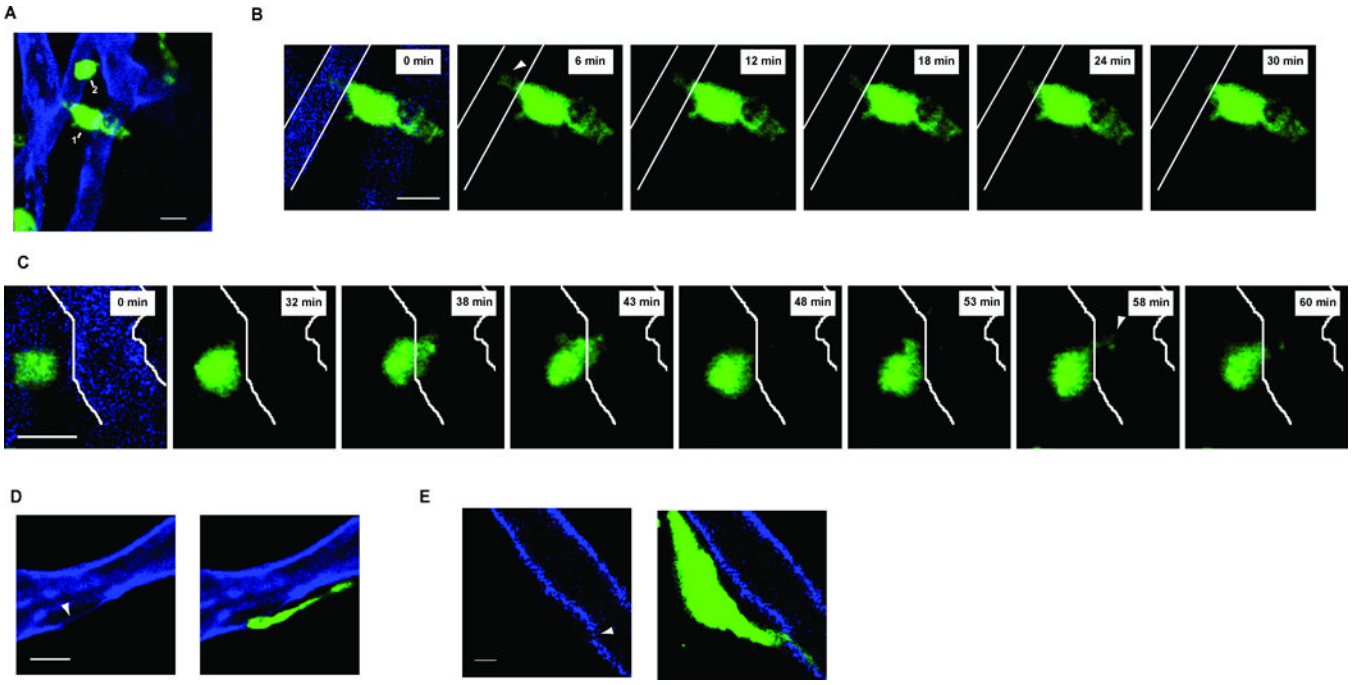

Figure 5. Mast cells are tightly associated with blood vessels and can dynamically sample the intravascular lumen

A. A 25 μm maximum intensity projection of two mast cells (green and labeled 1 or 2). Both mast cells are adjacent to blood vessels (blue). The scale bar is 10 μm. z-stack is representative of imaging performed on three individual mice.

B. Single z-slices of Cell 1 in A) starting at time 0 on the left. The boundaries of the blood vessel are then depicted only as white solid lines for the remainder of the z-slices. Each frame is separated by ~6 minutes and shows the withdrawal of the projection observed at time 0 and highlighted by the white arrowhead in the first slice.

C. Single z-slices of Cell 2 in A) starting at time 0 on the left. The boundaries of the blood vessel are then depicted only as white solid lines for the remainder of the z-slices. Each frame is separated by ~5 minutes and shows serial interactions between the mast cell and blood vessel with portions of the mast cell body in the vessel lumen at (t= 38 and 43) or a projection directed into the vessel at t=58).

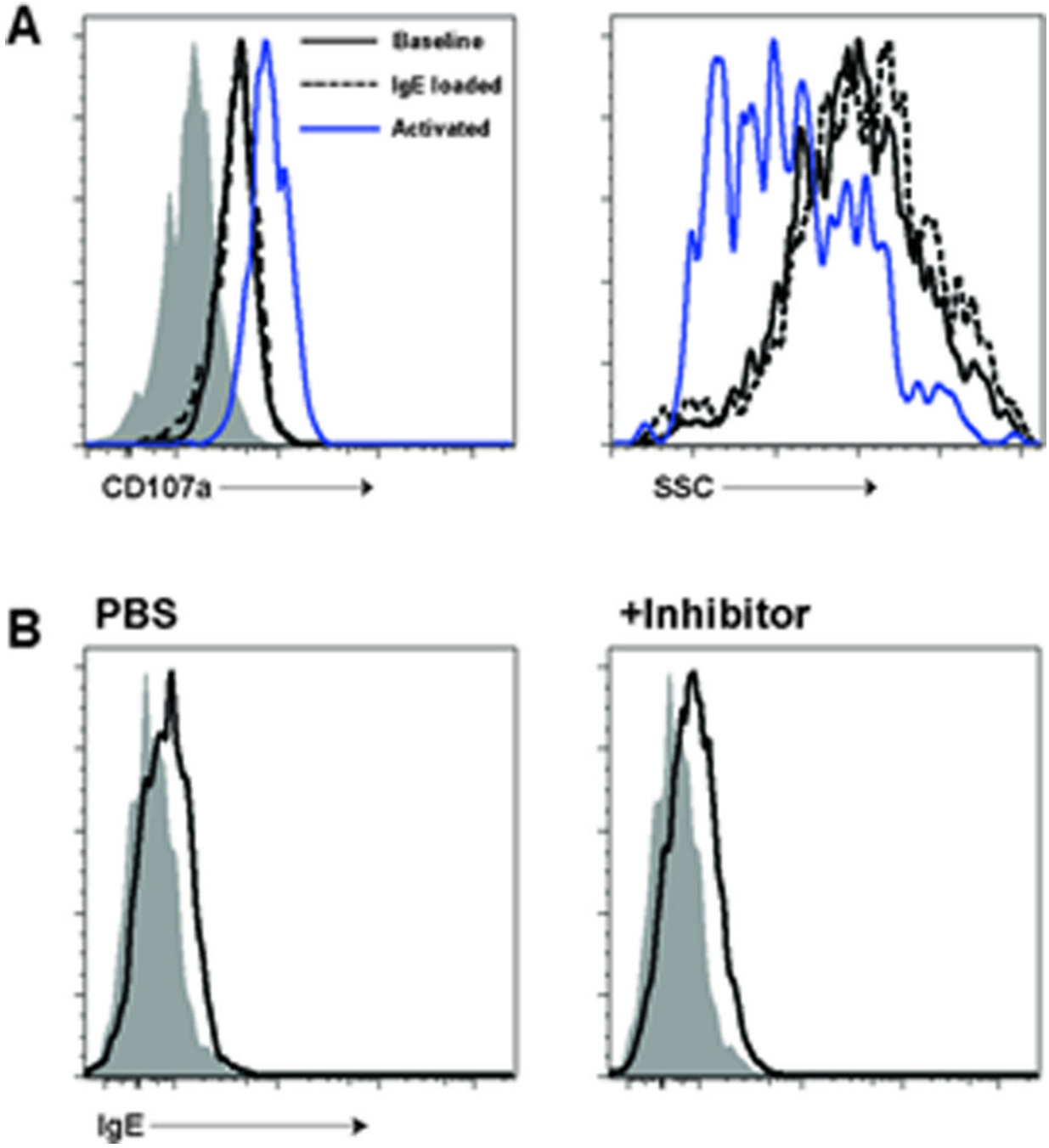

Figure 6. IgE loading does not cause degranulation and is unaffected by pharmacologic inhibition of mast cell function

A. 4get BALB/c mice received either PBS (solid black line) or monoclonal anti-TNP IgE antibody (dashed line) I.V. Four hours later, surface LAMP-1 (CD107a) and granularity (side scatter) were examined on peritoneal mast cells. An additional control group for mast cell activation is represented by the purple line. This group of mice had been loaded with anti-TNP IgE one day prior and challenged with 1 mg of TNP-ovalbumin at the start of the experiment. These activated mast cells demonstrate increased LAMP-1 staining after activation as well as a drop in side-

scatter (SSC). By contrast, IgE-loaded mast cells show equivalent LAMP-1 and SSC profiles compared to controls. The gray histogram in the left panel represents isotype control staining.

B. 4getxRag2$^{-/-}$ mice were pre-treated with PBS (left panel) or a combination of pyrilamine, ranitidine, and cromolyn sodium (right panel). Mice were then loaded with 10 μg of monoclonal IgE antibody and ear mast cells assessed for IgE uptake 24 hours later. No difference in IgE uptake was observed between the two samples.

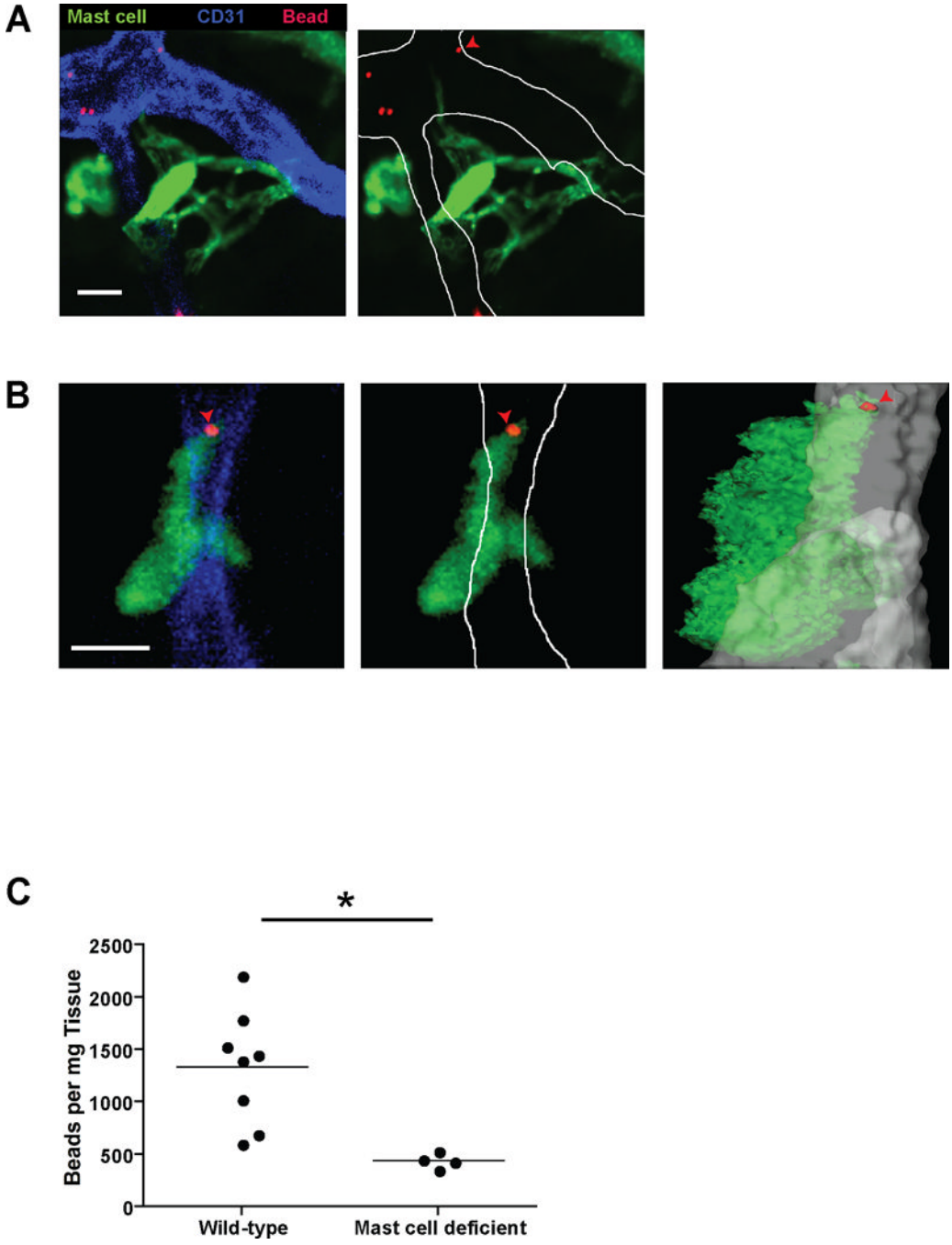

Figure 7. Mast cells capture intravascular IgE-coated beads

A. A single z-slice depicting a mast cell (green) directing projections into a blood vessel (blue) but not interacting with fluorescent beads (red). Ten minutes prior to imaging, the M5cre × Ai6 mast cell reporter mouse received ~10^9 rhodamine coated beads I.V. Scale Bar is 10 μm. The left panel shows the native image while the right panel highlights the boundaries of the vessel with improved visualization of the projections. Images are representative of 5 individual imaging volumes. One of the IgE beads is also denoted by a red arrowhead.

B. A single z-slice illustrating a mast cell (green) directing projections into a blood vessel (blue) and interacting with an IgE bead (red) distally. The IgE bead is also denoted by the red arrowhead. Ten minutes prior to imaging, the M5cre × Ai6 mast cell reporter mouse received ~10^9 IgE and rhodamine coated beads I.V. The left panel shows the native image while the middle panel highlights the boundaries of the blood vessel. The right panel is an orthogonal view of the z-stack. The mast cell (green), bead (red), and blood vessel (gray) have been transformed into surfaces. Scale Bar is 10 μm. Images are representative of 5 individual imaging volumes.

C. ~10^9 IgE coated beads were infused I.V. into wild-type or mast cell deficient (M5creDTA) mice and subsequently isolated from ear tissue after weighing. The number of beads is represented as the number of beads per mg of ear tissue. *$p<0.01$